Egyptian Journal of Chemistry

http://ejchem.journals.ekb.eg/

Enhanced anticorrosion properties of water-borne anticorrosive paints based on Zinc/magnesium/nanocarbon (Zn/Mg/NC)

[*1]Noha Elhalawany, [2]Jack Serour, [3]Amal M. Abdel-karim, [2]Maher M. Saleeb, [4]Fatma Morsy.

*[*1] Polymers and pigments dept., National research centre, 12622, Egypt*
[3]Physical chemistry dept., National research centre, 12622, Egypt
[2]Eagle Chemicals Company, Industrial Zone # 2, Part No. 233, 6th October, Egypt
[4]Chemistry dept., Faculty of science, Helwan University, Egypt
*[*1] corresponding author NohaElhalawany emails:*

Abstract

Zinc (Zn) and magnesium (Mg) network structures have been prepared chemically in presence of stable aqueous dispersion of nanocarbon (NC) to form the corresponding hybrid sol gel (HSG) of Zn /Mg /NC. Morphological studies and particle size distribution of the formed (HSG) have been determined via SEM/EDX, TEM and dynamic light scattering (DLS) respectively. The prepared (HSG) of different weight percent (3, 6, 9, 12 %) has been incorporated into ecofriendly anticorrosive water born paint formulations to protect carbon steel from corrosion. The painted metal panels have been tested for degree of rusting and blistering resistance in accordance with ASTMD. The physico-mechanical properties of the coated panels have been also investigated. The effect of the prepared HSG in enhancing corrosion protection efficiency IE% of the painted panels has been monitored by potentiodynamic polarization and electrochemical impedance spectroscopy. The results revealed that as the concentration of the prepared HSG increases as the IE% increases. Maximum inhibition efficiency IE% up to 96.5% was obtained. As far as we know, these featured corrosion resistances for the prepared paint formulations have not been reported yet in the open literature.

Key words : Nanocarbon, hybrid sol gel, anticorrosive water born paints and corrosion protection.

1. Introduction

Organic coatings are the most proper system to protect steel from corrosion where they provide a passive barrier layer between the steel substrate and corrosive species. Unfortunately, by time the corrosive species such as (O_2, H_2O and Cl^-) can reach to the metal/coat interface due to porosity leading to formation of hydroxyl ions which causes blistering. Therefore, organic coatings have weaknesses and cannot afford efficient corrosion protection [1, 2]. Numerous approaches have been established to enhance corrosion protection using organic coatings [3-5]. One of the numerous approaches is to incorporate additives such as fillers, pigments and nanoparticles into the organic coatings. In this context, various additives and pigments such as zinc aluminum phosphate [6], conducting polymers nanoparticles [7], SiO_2 [8], chromium compounds [9] and graphene oxide (GO) nanosheets [10] have been used. It was discovered that these additives highly enhanced the barrier characteristics of the organic coating and hence the anticorrosion properties.

Till today chromium (VI) containing coatings is one of the ultimately used methods. Due to the toxicity of chromium (VI) compounds, coatings containing chromium are unfavorable for metal protection [9]. An appropriate substitute of chromium (VI) coating is so far to be explored.

A challenging echo friendly sol–gel coating is an emerging way to protect steel from corrosion compared with the conventional chromate and phosphate containing coatings. The quick evolution of sol gel technology comes from the excellent chemical stability, oxidation control and enhanced corrosion resistance for metal substrates [11]. Sol–gel coatings and their applications have been broadly studied [12].

*Corresponding author e-mail: *elhalawany1933@gmail.com-nohaelhalawany1@yahoo.com*
Receive Date: 20 June 2021, Revise Date: 13 July 2021, Accept Date: 04 August 2021
DOI: 10.21608/EJCHEM.2021.81631.4037

Lastly, the sol gel derived coatings have been used to protect aluminum and steel metal surfaces [13].

A sol–gel coating can be applied to a metal substrate through various techniques, such as dip-coating and spin-coating, which are the two most commonly used coating methods. After film formation, cracks have been formed due to the evaporation of solvents and water which causes internal stresses leading to the deterioration of the formed film.

Recently, organic–inorganic hybrid (OIH) gels of functionalized trialkoxysilanes have been used to protect metal surfaces from corrosion [14]. (OIH) coatings are of distinctive interest due to their collective properties of organic and inorganic materials [15-17]. It was found that, the presence of organic components in sols reduces coating porosity due to dense film formation [18]. The presence of organic groups such as methyl groups in RO-Si -OR and perfluoro groups that have low surface tension in comparison with inorganic oxides can help in forming hydrophobic surfaces during the drying process [19].

As far as we know, these water born anticorrosive paint formulations have not been reported yet in the open literature hence, an attempt has been made to prepare ecofriendly anticorrosive paints based on the prepared novel (HSG) of different Wt. % as corrosion inhibitor for carbon steel protection. The painted carbon steel panels have been tested for corrosion via the degree of rusting and blistering resistances in accordance with ASTMD. Potentiodynamic polarization and electrochemical impedance spectroscopy (EIS) measurements in a corrosive environment (3.5 wt. % NaCl) for the painted carbon steel panels have been determined.

2. Experimental

2.1 Materials

Magnesium chloride $MgCl_2$, Zinc acetate $(CH3COO)_2$ Zn, and dodecyl benzene sulfonic acid (DBSA) were supplied from Sigma–Aldrich Company, USA. Commercial carbon black (CB) is supplied from rubber workshop at National research center, Cairo, Egypt. Butyl acrylate and acrylic acid monomers were products of Sigma Aldrich, USA. Titanium dioxide (under the trade name rutile R-902 is the product of Du-pont Company, Wilmington, USA) and it was used as the main pigment. Sodium acetate and ammonia are products of (Target Chemicals Company, Cairo, Egypt, 98%) and (CHIMI ART Chemicals Company, Cairo, Egypt) respectively and were used as pH stabilizers. Tylose (under the trade name Tylose® H 30000 YP2) is product of GmbH & Co. KG Company, Kapfenberg, Austria) and was used as a thickening agent. Calcium carbonate is product of the ACMA for chemicals and mining, Egypt. Texanol(2,2,4-trimethyl-1,3-pentanediol mono iso butyrate), WD-EAGLE (AS 40/40) and tetra potassium pyrophosphate are products of (Eastman Chemical Company, Melbourne, Australia), (Eagle Chemicals Company, 6th October, Egypt, solid content 45%) and (Energy Chemical Company, China) and were used as coalescing, dispersing and wetting agents, respectively. AGITAN 301 is used as an anti-foaming agent and is product of (MünzingChemie, Germany, solid content: 100%). Acticide HF, the antibacterial agent was purchased from Clariant International Ltd., Muttenz, Switzerland.

2.2. Methods of preparations

2.2.1. Synthesis of Nano carbon (NC) colloidal solution

A stable nanocarbon NC transparent aqueous dispersion has been prepared by mixing carbon black CB and dodecyl benzene sulfonic acid DBSA of ratio (1:1) in 80 ml water under continuous vigorous stirring for 10 min till transparent aqueous dispersion was obtained as shown in Fig.1.

Fig1: Stable aqueous dispersion of NC

2.2.2. Synthesis of hybrid sol gel of Zn/Mg/NC:

A stable hybrid sol gel of Zn/Mg/NC has been prepared by mixing Zn^{+2}/ Mg^{+2} salt solutions of ratio (1:1) in presence of the aforementioned NC solution under continuous vigorous stirring for 10 minutes followed by the addition of one drop of concentrated HCl under continuous stirring till the homogeneous greyish white colloidal solution was obtained. The formed colloidal solution was then centrifuged, washed several times by dist. water and finally redispersed in dist. water for further use.

2.2.3. Preparation of Pure Acrylate emulsion

Semi-continuous emulsion copolymerization of butyl acrylate and acrylic acid monomers has been carried out at eagle chemical company according to Elhalawany et al [8]. The copolymerization reaction has been carried out under N_2-gas conditions

conferring to the recipe shown in Table 1. The produced latex was filtered, cooled below 30°C and then kept for further use. The specifications of the produced latex are listed in Table 2.

Table1: Acrylate emulsion polymerization recipe.

Raw materials	Weight (gm)
Initial reactor charge	
De-ionized water	980
Sodium acetate	3.1
CAFLON NAS-30 S	7.3
Monomers Mixture (4 hours feed)	
Acrylic Acid	100
n-Butyl Acrylate	1000
Initiator Mixture (4 hours feed)	
APS	1
De-ionized water	97.7

Table 2 : Acrylate emulsion specifications.

Acrylate emulsion specifications			
Viscosity	100-500 cP	**pH**	7-9
Solid content	50%	**Film properties**	Clear, glossy and transparent
Density	1.05 kg/L	**Minimum film forming temp. (MFFT)**	15 °C
Average M wt.	250,000	**Tg**	18

2.3. Characterization of the prepared materials:

Scanning electron microscope (SEM/EDX): SEM for the prepared NC and the formed HSG has been measured using FE-SEM (QUANTA FEG250), at High Voltage (20KV) at SEM lab, Central Service Labs, (NRC), and Cairo, Egypt. **Transmission electron microscope (TEM):** The morphological studies of the prepared materials have been determined via transmission electron microscope TEM + DEM Jeol-JEM 1230, Japan at Electron Microscope lab, Physics department, NRC, Cairo, Egypt. It works at 120 KV; magnification power is ×600 k and resolution until 0.3 nm. **Dynamic light scattering (DLS):** The particle size distribution as well as zeta potentials have been determined using a Zetasizer from Malvern Instruments, England (model3000-HS).

2.4. Paint preparation:

White coatings have been prepared successfully from the prepared acrylate emulsion (binder) and the prepared HSG of Zn/Mg/NC (corrosion inhibitor) of different Wt. %. These coatings have been used for preparing paint films for all tests. Three substrates, (steel, tin and glass panels) have used for all measurements. These substrates were purified carefully and dried before use. The surface of carbon steel was polished and cleaned for the purpose of electrochemical measurement. All paints were applied on the panels by using a suitable film applicator to get uniform film thickness and dried at 25 °C for 1 week.

2.5. Physico-mechanical properties:

The gloss of paint films has been measured using Spectromatch Gloss 45/0◦ from Sheen Instruments Company in accordance with ASTM D 523-08. Mandrel-Bending tester from BYK-Gardner Company was used to measure a range of elongation of a dry paint film in accordance with ASTM D 522-93a (2008). The hardness of paint was evaluated with Pendulum Hardness Rocker tester; model 707 KONIG from Sheen Instruments in accordance with ASTM D 4366-95 (2003). The adhesion power of paint film to the base substrates was tested using the cross-cut test instrument – Sheen Company in accordance with ASTM D 3359-09e2. Using CHOC Variable-Impact Tester from – Braive Instruments, to measure resistance of organic coatings to the effects of rapid deformation (Impact) in accordance with ASTM D 2794-93 (2010).

2.6. Corrosion studies:

The corrosion tests have been carried out with hand-made **equipment** established in Research and Development Department, Eagle Chemicals Company, Egypt [8] where the scratched painted steel plates have been stored in an aqueous solution of NaCl (3.5 wt. %, pH 6.6) in presence of artificial air bubbles up to 28 days. After 28 days the plates have been washed with distilled water and dried. The plates have been then detected for degree of rusting and blistering in accordance with ASTM D 610 (2001) and ASTM D 714–87 (2000) respectively.

2.7. Electrochemical measurements:

Electrochemical corrosion studies of the painted carbon steel plates have been carried out in a three-electrode cell via Autolab potentiostat/galvanostat PGSTAT302N connected to a computer. Ag/AgCl is considered as reference electrode and Pt is the counter electrode. The uncoated carbon steel (UCS), Blank (free from HSG) and coated carbon steel plates with the different paint formulations of (3%HSG, 6%HSG, 9%HSG and 12%HSG) are all considered as working electrodes immersed in an electrolyte solution of 3.5% NaCl of exposed area of 1 cm^2. The potentiodynamic current-potential curves have been monitored by changing the electrode potential automatically from −800 mV to 0 mV with a potential scan rate of 1 mVs^{-1}. The corrosion parameters such as corrosion

current density i_{corr} and corrosion potential E_{corr} have been determined from the intersection of the linear anodic and cathodic branches of the Tafel plots. Electrochemical Impedance Spectroscopy (EIS) has been attained in the range from 10 MHz to 100 kHz with an Ac voltage amplitude of 10 mV. All the electrochemical measurements have been done at open circuit potential. The values of the potentiodynamic parameter and equivalent circuit parameters have been investigated by Nova 1.11 software.

3. Results and Discussion

The aim of this work is to prepare a novel hybrid sol gel (HSG) of zinc and magnesium in presence of stable aqueous dispersion of NC for use as corrosion inhibitor in ecofriendly water-born anticorrosive paints for carbon steel surfaces protection.

In this study, stable nanocarbon NC aqueous solution has been prepared by exploiting the strong crushing and degradation effects of the high shearing effect homogenizer and the radical trapping nature of CB to break the large agglomerates of CB and to support the grafting of the anionic surfactant DBSA onto it [20, 21]. While homogenization, the large aggregates of CB will be broken down and surrounded by the anionic surfactant to prevent agglomeration leading to the formation of homogeneous stable transparent aqueous dispersion of NC. Mg and Zn network structures have been formed in presence of the prepared a stable aqueous dispersion of NC via sol gel technique according to the following equations:

$M^{2+} + H_2 \Rightarrow$ M-OH (hydrolysis) ------ eq1

M-OH + M-OH $\Rightarrow$ M-O-M $+H_2O$ (Condensation) eq2

Where, M^{2+} represents (Mg^{2+} or Zn^{2+}) ions. A plausible mechanism for the formation of the HSG is represented in Fig. 2

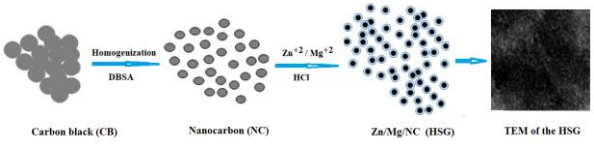

Fig.2: Formation of the hybrid sol gel of Zn/Mg/NC.

3.1. Characterization:

3.1.1. TEM analysis for the prepared hybrid sol gel:

Figure 3a, b shows the TEM micrograph of the prepared NC and the formed hybrid sol gel HSG. It is clearly seen from the Fig.3a that the nanocarbon particles are homogeneously dispersed and have semigraphitic nanostructures in the size range from 29 to 40 nm.

Fig. 3b shows that the nanoparticles of the formed HSG have taken core shell structures where the darker spots are related to NC forming the core and the lighter shells are related to Mg/Zn network structures.

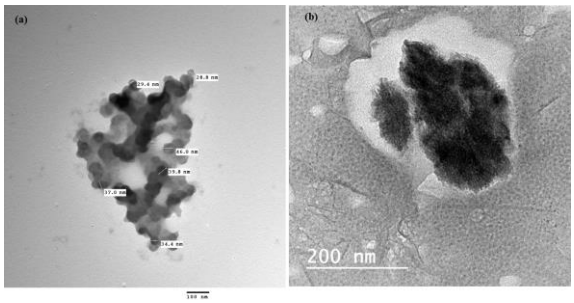

Fig. 3: TEM micrograph of the prepared a) NC and b) HSG.

3.1.2. SEM/EDX analysis of the prepared hybrid sol gel:

Fig. 4 a,b shows the SEM micrograph and the energy dispersive x-ray analysis (EDX) for the formed HSG. It is clearly seen from Fig. 4a that the prepared HSG showed compatibility with a very tiny pore size indicating good covering for surfaces as proposed. Fig. 4b shows the EDX analysis of the prepared HSG. The incident x- ray beam will excite an electron in the inner shells of the atoms leading to the ejection of an electron from the shell while creating an electron hole. An electron from the outer energy levels, will then fills the hole, and the difference in energy between the outer-energy level and the inner energy level will be released in the form of an X-ray which is characteristic for each element. Fig. 5b showed peaks at 0.277, 0.025, 8.63 and 1.25 eV which are characteristic for carbon, oxygen, Zn and Mg respectively.

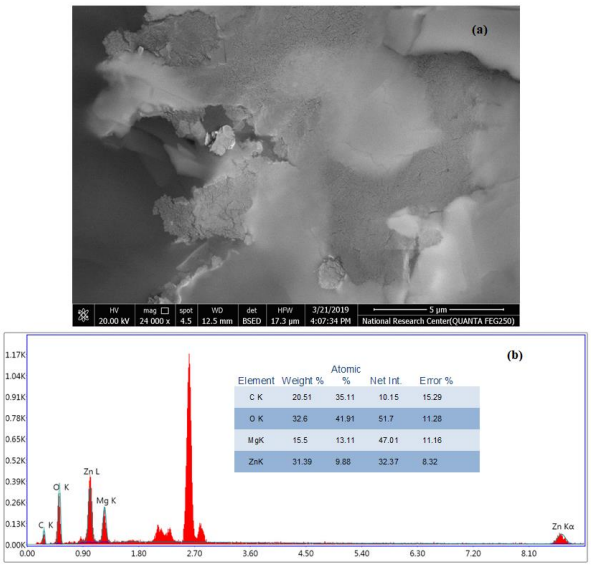

Fig. 4: (a) SEM micrograph and (b): EDX analysis of the prepared HSG.

3.1.3. Particle size distribution:

Fig.5 shows the particle size distribution of the prepared nanocarbon (NC) using dynamic Light Scattering. This technique uses monochromatic light beam to hit the liquid of globular particles in Brownian motion leading to changing in the wavelength of the

received light. This change is correlated to the size of the particle. Fig. 5 showed one broad peak for the formed NC with size ranges between 100-300 nm. Diameters obtained from DLS measurements are not essentially the correct dimension of the dispersed relevant particles; but it is a hydrodynamic diameter of a sphere dispersing at the same rate as the particles [22]. Fig. 6a, b shows the particle size distribution and the zeta potential of the formed HSG. It is clearly seen from Fig. 6a that the particle size distribution has one narrow peak indicating homogeneity of the formed HSG with sizes in the range from 168 to 350 nm. Fig. 6b shows zeta potential distribution for the formed HSG. Zeta potential is a scientific term which expresses to electro-kinetic potential. The importance of zeta potential is that it is correlated to the stability of the colloidal solutions. The zeta potential expresses the degree of repulsion between adjacent, likely charged particles. As the particles are small enough, the liquid dispersion will resist agglomeration indicating stability and higher zeta potential will be obtained. When zeta potential is low, attraction surpasses repulsion and the dispersion will agglomerate. Consequently, dispersion with high zeta potential (negative or positive) is electrically stabilized while that of low zeta potentials tend to agglomerate. It is shown from Fig. 6b that the zeta potential is high enough which indicates that the formed HSG is electrically stabilized.

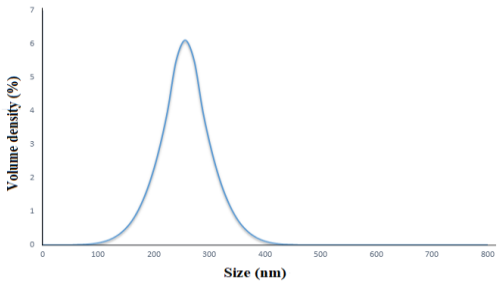

Fig. 5 : Particle size distribution of the formed NC.

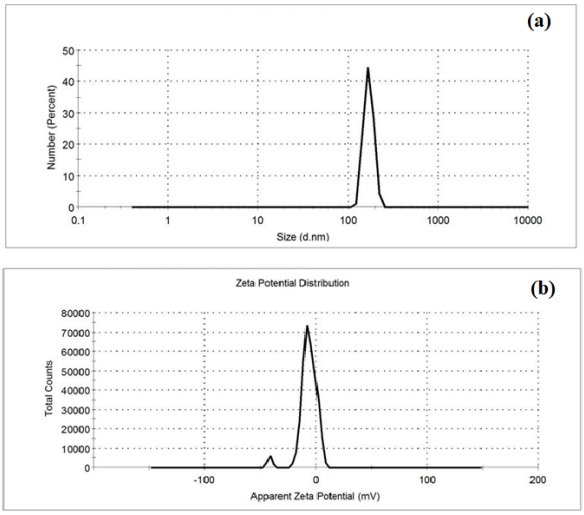

Fig. 6: (a) : particle size distribution and (b) Zeta potential distribution for the prepared HSG.

3.2. Anticorrosive water based paint formulations:

The binder used in the present study is polyacrylate PA emulsion (butylacrylate/acrylic). The PA emulsion of solid content (50%) has been mixed with the prepared hybrid sol gel HSG of different weight percent (3%, 6%, 9% and 12%) and incorporated into paint formulations forming the corresponding coatings or paints of (3%HSG, 6%HSG, 9% HSG and 12%HSG). Table 3 shows the paint formulations for blank sample (free from the prepared HSG) and the paint formulations containing the HSG of different wt. %.

Table 3: paint formulations.

Composition	Blank	3 % HSG	6 % HSG	9 % HSG	12 % HSG
Water	250	242.5	235	227.5	220
Tetra potassium pyrophosphate	2.5	2.5	2.5	2.5	2.5
WD-EAGLE (AS 4/40)	4	4	4	4	4
Texanol	14	14	14	14	14
AGITAN 301	6	6	6	6	6
Tylose H30,000	6	6	6	6	6
Ammonia	2.5	2.5	2.5	2.5	2.5
Titanium dioxide	210	210	210	210	210
PA (binder)	100	100	100	100	100
HSG	------	7.5	15	22.5	30
Acticide HF	5	5	5	5	5
Calcium carbonate	400	400	400	400	400
Total (g)	1000g	1000g	1000g	1000g	1000g

3.3. Physico-mechanical tests

The physico-mechanical test results of the painted films containing the prepared HSG and blank films are tabulated in Table 4. It is shown from the results tabulated in Table 4 that the presence of the HSG hasn't affected much on adhesion, hardness and pending properties of the final paint while the washability has been affected much by the increase in the Wt.% of the prepared HSG.

3.4. Corrosion resistance test

To examine the corrosion resistance, different steel panels have been painted with the prepared paint formulations. After drying the painted films for one week, they have been immersed in artificial seawater for 28 days. The corrosion tests results are given in Table 5. The corrosion progress on metal plates under paint films of the blank and HSG containing samples is represented photographically in Fig. 7 and tabulated in Table 5. Maximum failure was obviously obtained for the blank sample, where severe corrosion (rating 7) and 3D blisters rating were observed as shown from Fig.7 and Table 5.

Table 4: Physico- mechanical properties of the prepared paint films.

Test	Blank	HSG			
		3%	6%	9%	12%
Adhesion , dimensionless	2B	2B	2B	1B	1B
Hardness , cycle(the number of cycles by pendulum hardness machine which can penetrate the paint film)	50	50	52	51	52
Bending , dimensionless(the flexibility of the final paint)	Pass	Pass	Pass	Pass	Pass
Gloss and whitness 60°/85° after one week (the gloss and whiteness of the dry films)	2.4/17.3	2.3/18	2.4/19.3	2.2/17	2.2/18.2
Washability, cycle (the number of cycles required to erode the paint film by a Bruch)	more than 3000	3000	more than 3000	2000	500

1B (less than 35-65% of the area is affected
2B(less than 15-35% of the area is affected

Table 5: Corrosion resistance tests of the coated steel panels.

Tests	Blank	HSG			
		3%HSG	6% HSG	9% HSG	12% HSG
Degree of rusting Rating of rust as area percentage (scale from 10 to 0, where 10 < 0.01% and 0=100%)	5	6.5	8	9	9.5
Degree of blistering Where F, M, MD and D are (few, medium, medium dense and dense) respectively.	D	MD	M	F	F

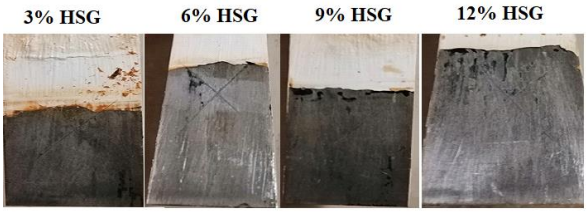

Fig. 7: Corrosion test of steel panel coated with Bank and the prepared anticorrosive paint formulations containing different wt. % of the prepared HSG.

As shown from Fig. 7 and data given in Table 5, the corrosion resistance of the steel panels painted by the prepared paint formulations containing the (HSG) increases as the wt. % of the HSG increases. The enhanced corrosion protection observed for samples containing different weight percent of the HSG is attributed to the combination of galvanic protection of the present Zinc and Magnesium network structures as well as barrier protection of the present NC.

The presence of Zn and Mg network structures will act as sacrificial anodes for carbon steel protection where naturally occurring

electrochemical potential difference between the different metallic elements arises [23].

3.5. Potentiodynamic polarization Measurement:

The corrosion behavior of the coated samples has been measured via linear Potentiodynamic polarization in corrosive environment (3.5% NaCl). Fig. 8 Shows the Tafel polarization plot of uncoated metal plate (UCS), coated metal plate by blank paint formulation (free from the HSG) and coated plates by the prepared paint formulations (3%, 6%, 9% and 12% HSG) in corrosive environment (3.5 wt. % NaCl solution). It is obvious that all plots of the coated samples by the prepared paint formulations are shifted to less negative potential with increasing the wt. % of the HSG. The passivation effect has been reported and it was detected that the corrosion potential of blank sample has higher negative value of - 0.659V than that of paint formulation (12% HSG) which tends to less negative value of -0.555 V. This shift to less negative value i.e more positive potential indicates that the dissolution resultant from corrosion was decreased. The large anodic shift monitored confirms the anodic protection [24], indicating that these paint formulations perform like a barrier by reducing the capability of corrosion.

Corrosion potential (E_{corr} vs. Ag/AgCl), corrosion current density (I_{corr}), polarization resistance (R_{pol}), and Tafel slopes anodic β_a and cathodic β_c are the electrochemical polarization parameters have been calculated and listed in Table (6). It is evidently seen from the results that the current density has shifted to lower values from $2.49x10^{-4}$ A/cm^2 for UCS to $9.65x10^{-5}$A/cm^2 for blank and to $2.15x10^{-6}$ A/cm^2 for 12 % HSG coated sample. This decrease in the corrosion current density expresses to the effective protection performance of the prepared paint formulations containing the HSG against corrosion. Fig. 8 showed also that both the anodic and the cathodic branches are shifted to lower current density region, signifying that the painted film can regulate both the anodic and the cathodic reactions. As the wt. % of the HSG in the prepared paints increased as the corrosion resistance of the coatings increased in the range from 363 to 13527 ohm. The corrosion rate decreases also with an increase in the wt. % of the prepared HSG indicating the increase of corrosion protection. Commonly, the blank paint has a lot of micropores which give the chance for the corrosive species to penetrate easy; however the presence of HSG of different wt. % may block these pores, resulting in enhancement of coating homogeneity. NC may have barrier effect resulting in the improvement of coating compactness and hence more corrosion protection. . In addition to, the galvanic protection of the present Zn and Mg network structures which act as sacrificial anodes [23].

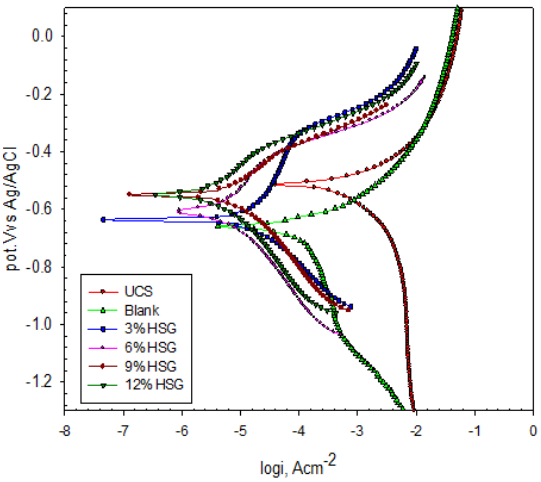

Fig. (8): Tafel polarization curves of uncoated metal surface (UCS) and coated metal surfaces by blank and the prepared paint formulations of different wt. % of HSG.

The corrosion of carbon steel under conditions of water and air access can be written as follows:

$$2Fe + O_2 + 2H_2O \longrightarrow 2Fe(OH)_2 \text{ -------- eq3}$$

The resultant, ferrous hydroxide was further oxidized to form magnetite (Fe_3O_4) or a hydrated ferric oxide (FeOOH), which is known as rust. It is appropriate to consider separately the anodic and cathodic reactions as represented in equations 4, 5 as follows:

$$2Fe \longrightarrow 2Fe^{2+} + 4e \text{ ----------eq4}$$

$$O_2 + 2H_2O + 4e \longrightarrow 4OH^- \text{ ------- eq5}$$

One can conclude that corrosion is a chemical reaction occurring by an electrochemical mechanism. Presence of Zn and Mg network structures will act as sacrificial anodes for carbon steel due to the naturally occurring electrochemical potential difference between Zn, Mg and iron metals. Zn and Mg alloys are the best frequently used sacrificial anodes [23].

The corrosion protection efficiency (IE %) can be deduced from the Tafel parameters according to the following equation [25]:

$$IE\% = \frac{i_{uncoated} - i_{coated}}{i_{uncoated}} x100 \quad --- eq6$$

Where, i (uncoated) and i (coated); are the corrosion current densities for uncoated and coated specimen respectively.

Blank sample showed 62.11% protection efficiency while 12 % HSG paint sample showed higher value of 99.3%. The corrosion rate of the steel panels comes in reverse with the efficiency data where the highest protection gave the lowest corrosion rates as shown in Fig 9. The lower corrosion protection of blank sample may be attributed to the porosity of the coating.

Table 6: Polarization parameters of uncoated and coated carbon steel in 3.5 % NaCl

Concentration	$E_{corr.}$(V) vs. Ag/AgCl	b_a (V dec^{-1})	b_c (V dec^{-1})	$I_{corr.}$ ($A.cm^{-2}$)	R_P ($\Omega.cm^2$)	*C. R.* (mm/year)	*I E* (%)
UCS	-0.512	0.117	0.064	$2.49x10^{-4}$	72	2.890	------
Blank	-0.659	0.349	0.114	$9.65x10^{-5}$	363	1.120	62.11
3% HSG	-0.636	0.189	0.122	$9.16x10^{-6}$	3517	0.110	96.18
6 % HSG	-0.612	0.269	0.191	$4.98x10^{-6}$	9753	0.060	97.9
9 % HSG	-0.549	0.140	0.134	$4.62x10^{-6}$	6447	0.053	98.15
12 % HSG	-0.555	0.162	0.114	$2.15x10^{-6}$	13527	0.020	99.30

The presence of Zn/Mg/NC nanoparticles which entrapped in polyacrylate PA emulsion binder provide reinforcement to the PA chains, which reduces the degradation of the polymer chains in acidic environment by filling the pores leading to high protection against corrosion. The corrosion studies showed that the coatings containing the prepared HSG showed much better corrosion protection than blank coating (free from Zn/Mg/ NC). The sample containing 12 wt. % of the HSG has maximum corrosion protection due to the lower current density and the lower corrosion rate. This confirms that the paint coatings containing the HSG have much better corrosive resistance than that of the free coating [26]

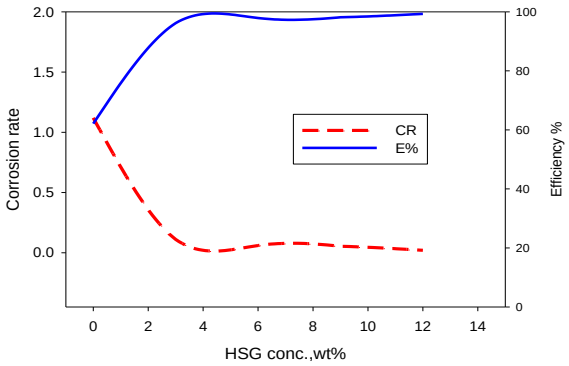

Fig.(9) The change of the corrosion rate and the coating efficiency from polarization curve versus the wt.% of the HSG.

3.6. Electrochemical Impedance Spectroscopy (EIS) Measurements:

EIS is the most fruitful application to evaluate the properties of the coated metals. It should be noted that the impedance is the resistance when a current passes through a circuit comprising resistors and capacitors [26]. The electrochemical performance of UCS and all painted samples in 3.5% NaCl solution has been evaluated using electrochemical impedance spectroscopy Nyquist and pode plots.

The Nyquist impedance charts are represented in Fig. 10. The diameter of the capacitive loop represents the charge transfer resistance. The capacitive loop for coated metal is much larger than that of UCS and increases as the wt. % of HSG increases. This increase is attributed to the coating film which prevents the destructive species to penetrate the film [27]. So the corrosion rate of the coated one is lower than that of UCS. These excellent anticorrosion properties can be ascribed to the spread of the prepared HSG nanoparticles in polyacrylate binder which reduce the rate of water and oxygen penetration [28] due to the dual effect of the galvanic protection as well as barrier effect of the Zn/Mg nanoparticles and NC respectively. The graph related to UCS has one time constant. However, the rest of the coated metal samples have two time constants in which the first one at high frequencies is correlated to the organic coating used and the second one at low frequencies is correlated to reactions occurring at the metal surfaces.

Fig. 11 represent the bode and phase plots where the horizontal axis show the frequency values in Hz and the vertical axis represents the impedance values in $\Omega.cm^2$ and phase angle. As shown from Fig. 11 there are shifts in phase angle to lower frequency and the peaks become broader with increasing the wt. % of the HSG. By drawing the curves related to all samples under study in a Bode diagram, a reasonable comparison of the impedance values can be achieved. The Bode format displays resistive regions at high and low frequencies (HF and LF), where log |z| is tending to become constant (horizontal line) associated with phase angle value falling near to zero degree. At HF the solution resistance (R_s) is dominant, while at LF both R_s and R_c are the controlling parameters, where R_c is the coating resistance. The middle frequency (MF) range has noticeable capacitive response. According to previous researches [29], the sample that has higher impedance values at different frequencies is considered as the best for corrosion protection. So the prepared paints containing the formed HSG have the best protective properties.

The electrical equivalent circuit used to fit the experimental data of UCS and coated metal with 12% HSG are shown in Fig 12a,b. EIS parameter as R_s solution resistance, R_c coating resistance, R_{ct} charge transfer resistance, C_c capacitance of the coating and C_{dl} the double layer capacitance are listed in Table (7). Fig. 12c represents the fitting curves of UCS and the coated metal with 12 % HSG. Due to penetration of the corrosive species (electrolyte) through the coating a capacitive loop is obtained. In conclusion, once the electrolyte reaches the metal/paint interface, faradic processes occur and new loops are detected in the impedance spectra. Constant phase element (CPE) instead of a capacitive element is used to reach a more precise fit of experimental data which measures, n the

deviation from the ideal capacitive behavior. The higher capacitance value of UCS and Blank can be ascribed to less protection due to greater exposure of metal surfaces to aggressive corrosive species. The present HSG nanoparticles affect on the compactness of the coat by filling the pores of the coat forming barrier besides galvanic protection of Zn and Mg and hence prevent the diffusion of water and corrosive species through the coat leading to enhanced protection. It is clearly seen from Table (7) that the resistance of the barrier layer has converse drift with its capacitance i.e the higher the resistance the lower the capacitance is. The impedance and charge transfer resistance have increased to higher values under applied frequencies, while the CPE values decreased by increasing the wt. % of the HSG. The inhibition efficiency was calculated from the following equation [30]:

$$IE\% = \frac{RI_{coated} - R_{uncoated}}{R_{coated}} \; x100 \; --- eq7$$

It is seen that IE% increases with increasing wt. % of HSG and reached maximum value 96.5% for 12% HSG. It was found that the painted films by 12 % HSG paint formulation have shown enhanced performance, merging a number of promising properties such as smooth surface and homogeneous distribution ensuring a good adhesion of the film to the metallic substrate. This conclusion matches well with the results of linear polarization.

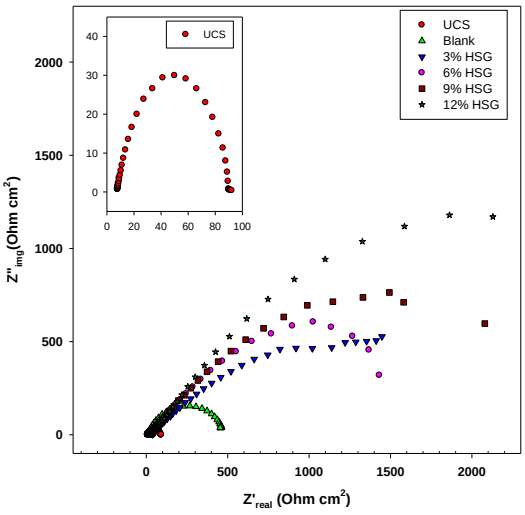

Fig. (10) Nyquist plot of uncoated and coated samples with paint formulations of different Wt. % of HSG.

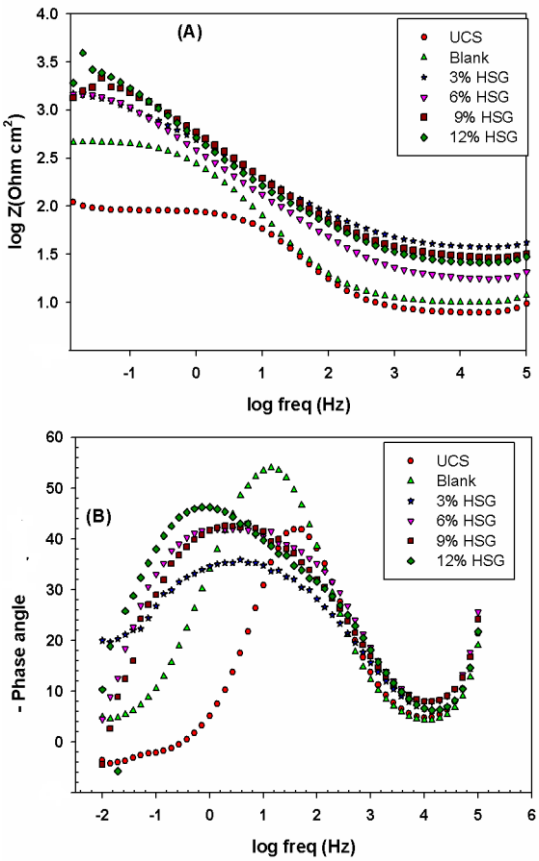

Fig. (11): (A) Bode (B) phase plot of UCS, Blank and coated samples with the prepared paint formulations of different wt. % of HSG.

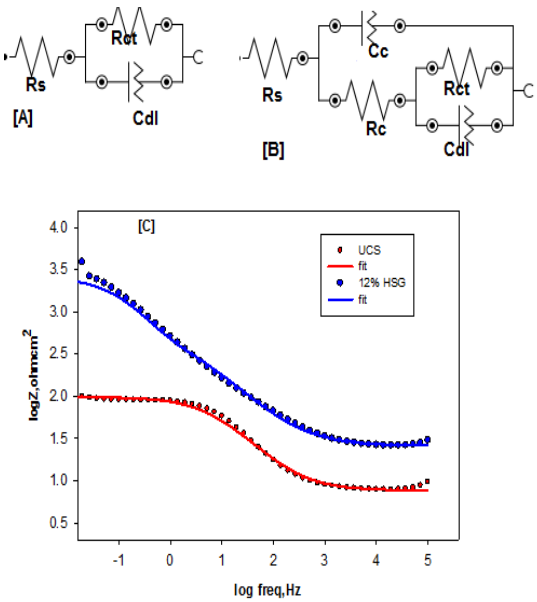

Fig. 12: Equivalent circuit models used for fitting of impedance [A] for uncoated surfaces UCS and [B] for coated surfaces and [c] Fit result of Bode plots of UCS and coated surfaces by 12% HSG paint formulation.

Table (7) EIS parameters of uncoated and coated carbon steel in 3.5 % NaCl

Concentration	*Rs* (Ω)	R_1 (Ωcm^2)	Q_1 ($\mu F\ cm^{-2}$)	*n*	R_2 (Ωcm^2)	Q_2 ($\mu F\ cm^{-2}$)	*n*	*IE %*
UCS	7.60	91.39	$8.78x10^{-4}$	0.69	----	--------	----	-----
Blank	9.03	20.89	$7.58x10^{-4}$	0.80	500	$6.62x10^{-4}$	0.79	82.5
3%HSG	38.8	174	$6.96x10^{-4}$	0.70	1250	$5.97x10^{-4}$	0.70	93.6
6 % HSG	17.4	220	$5.48x10^{-4}$	0.70	1400	$5.03x10^{-4}$	0.85	94.4
9 % HSG	28.3	440	$4.89x10^{-4}$	0.70	1605	$4.69x10^{-4}$	0.87	95.5
12 % HSG	23.2	630	$3.74x10^{-4}$	0.63	2000	$3.79x10^{-4}$	0.88	96.5

Conclusion:

Novel HSG of Mg/Zn/NC of different weight percent has been prepared for the first time via sol gel technique. The formed HSG has been characterized. Morphological studies revealed that the HSG is compatible and has core shell structure. The particle size distribution and zeta potential analysis showed that the formed HSG is chemically stable and the particle sizes are in the range of nanoscale. The formed HSG of different Wt. % has been incorporated into water based anticorrosive paint formulations. It was found that as the Wt. % of the HSG increases in the tested paint as the inhibition efficiency IE% increases. The effective corrosion protection is attributed to the dual effect of the prepared HSG where the NC acts as a barrier and prevents the corrosive species from penetration to the coat, while the Zn and Mg network structures are acting as sacrificial electrodes for the metallic carbon steel surfaces. As far as we know, these promising anti-corrosion properties for the prepared paint formulations have not been reported yet in the open literature. Finally one can conclude that the formed paints are of low cost, easy to process, and will open the gate for further development in paint technology.

Acknowledgement

The authors wish to thank Research and Development Department, Eagle Chemicals Company, 6th October City, Egypt for generous and sincere assistance toward carrying out some of the necessary investigations and analysis in this work.

Conflict of interest:

no conflict exists and the authors declare that they have no conflict of interest.

Funding:

No funding is available

Reference

[1] Bi H., Sykes J., An investigation of cathodic oxygen reduction beneath an intact organic coating on mild steel and its relevance to cathodic disbonding, *Prog. Org. Coat*., 87, 83–87 (2015)

[2] Alam M.A., Sherif E.-S.M. , Al-Zahrani S.M., Fabrication of various epoxy coatings for offshore applications and evaluating their mechanical properties and corrosion behavior, *Int. J. Electrochem. Sci.*, 8, 3121–3131(2013).

[3] Megahed M.M., Abdel Bar M.M., Abouelez E.S.M., El-Shamy A.M. , Polyamide Coating as a Potential Protective Layer Against Corrosion of Iron Artifacts, *Egyptian Journal of Chemistry* (2021)

[4] El-Shamy A.M., Abdel Bar M.M., Ionic Liquid as Water Soluble and Potential Inhibitor for Corrosion and Microbial Corrosion for Iron Artifacts, *Egyptian Journal of Chemistry* 64 (4), 1867-1876 (2021).

[5] Zohdy K. M., El-Sherif R. M., El-Shamy A. M., Corrosion and Passivation Behaviors of Tin in Aqueous Solutions of Different pH, *Journal of Bio-and Tribo-Corrosion* 7 (2), 1-7(2021).

[6] Naderi R., Attar M., The role of zinc aluminum phosphate anticorrosive pigment in protective performance and cathodic disbondment of epoxy coating, *Corros. Sci*. 52, 1291–1296 (2010)

[7] Elhalawany N.R.**,** Mossad M.A. and Zahran M.K. Novel water based coatings containing some conducting polymers nanoparticles (CPNs) as corrosion inhibitors. *Progress in Organic Coatings* 77, 725– 732 (2014).

[8] Elhalawany N.R., Saleeb M. M. and Zahran M. K., Novel anticorrosive emulsion-type paints containing organic/inorganic nanohybrid materials. *Progress in Organic Coatings* 77, 548– 556 (2014).

[9]. Twite R. L and Bierwagen G. P., Review of alternatives to chromate for corrosion protection of aluminum aerospace alloys, *Prog. Org. Coat*., 33, 91-100 (1998).

[10] Xia W., Xue H., Wang J., Wang T., Song L., Guo H., Fan X., Gong H., He J., Functionlized graphene serving as free radical scavenger and

corrosion protection in gamma-irradiated epoxy composites, *Carbon* 101, 315–323 (2016).

[11] Duhua W., and Bierwagen G.P., Sol–gel coatings on metals for corrosion protection. *Progress in organic coatings* 64 (4), 327-338 (2009).

[12] Flavia B., and ichelina Catauro M., Sol-Gel Technology to Prepare Advanced Coatings. *Photoenergy and Thin Film Materials* 321-378 (2019).

[13] Balgude D., and Sabnis A., Sol–gel derived hybrid coatings as an environment friendly surface treatment for corrosion protection of metals and their alloys. *Journal of sol-gel science and technology* 64 (1), 124-134 (2012).

[14] Canto, C. F., Prado, L. D. A., Radovanovic, E., & Yoshida, I. V. P. Organic–inorganic hybrid materials derived from epoxy resin and polysiloxanes: synthesis and characterization. *Polymer Engineering & Science 48*(1), 141-148 (2008).

[15] José, N. M., & Prado, L. A. S. D. A. Hybrid organic-inorganic materials: Preparation and some applications. *Quimica Nova 28*(2), 281-288 (2005).

[16] Moreira, S. D., Silva, C. J., Prado, L. A., Costa, M. F., Boev, V. I., Martín-Sánchez, J., & Gomes, M. J. M. Development of new high transparent hybrid organic–inorganic monoliths with surface engraved diffraction pattern. *Journal of Polymer Science Part B: Polymer Physics*, *50*(7), 492-499(2012).

[17] Sanchez, C., Julián, B., Belleville, P., & Popall, M. Applications of hybrid organic–inorganic nanocomposites. *Journal of Materials Chemistry 15*(35-36), 3559-3592 (2005).

[18] Zheludkevich, M. L., Serra, R., Montemor, M. F., Yasakau, K. A., Salvado, I. M., & Ferreira, M. G. S. Nanostructured sol–gel coatings doped with cerium nitrate as pre-treatments for AA2024-T3: corrosion protection performance. *Electrochimica Acta 51*(2), 208-217 (2005).

[19] Zhang, Y., Wang, H., Yan, B., Zhang, Y., Yin, P., Shen, G., & Yu, R., A rapid and efficient strategy for creating super-hydrophobic coatings on various material substrates. *Journal of Materials Chemistry 18*(37), 4442-4449 (2008).

[20] Noha Elhalawany, Jack Serour, Amal M. Abdel-karim, Maher M. Saleeb , Fatma Morsy. Novel Water-Born Anticorrosive Paints Based on Modified Nanocarbon(NC) Journal of Bio- and Tribo-Corrosion 7:144 (2021).

[21] El Halawany, N. R., & Salama, A. H. ,Synthesis, characterization and electrical properties of novel conducting copolymer-nanocomposites via minimemulsion polymerization technique, Egypt. *J. Chem*. *52*(4), 555-571(2009).

[22] Garden, A. L., Scholz, K., Schwass, D. R., & Meledandri, C. J. Optimized colloidal chemistry for micelle-templated synthesis and assembly of silver nanocomposite materials. *Colloids and Surfaces A: Physicochemical and Engineering Aspects*, *441*, 367-377(2014).

[23] Sundjono, G. P., & Nuraini, L., The Selection of Magnesium alloys as Sacrificial Anode for the Cathodic Protection of Underground Steel Structure. *International Journal of Engineering Trends and Technology (IJETT)*, *51*(2) (2017).

[24] Spinks, G. M., Dominis, A. J., Wallace, G. G., & Tallman, D. E., Electroactive conducting polymers for corrosion control. *Journal of Solid State Electrochemistry 6* (2), 85-100 (2002). .

[25] Abdel-karim A.M., Shahen, S., & Gaber, G. 4-Aminobenzenesulfonic acid as Effective Corrosion Inhibitor for carbon steel in hydrochloric acid. *Egyptian Journal of Chemistry* 64 (2), 825-834 (2021).

[26] Li, W., Tian, H., & Hou, B., Corrosion performance of epoxy coatings modified by nanoparticulate SiO_2. *Materials and Corrosion*, *63*(1), 44-53 (2012).

[27] Sumi, V. S., Arunima, S. R., Deepa, M. J., Sha, M. A., Riyas, A. H., Meera, M. S., Viswanathan S. Saji , Shibli, S. M. A. (2020). PANI-Fe_2O_3 composite for enhancement of active life of alkyd resin coating for corrosion protection of steel. *Materials Chemistry and Physics 247*, 122881 (2020).

[28] Hang T.T.X., Truc T.A., Nam T.H., Oanh V.K., Jorcin J.B., and ´eb`ere N.P., Corrosion protection of carbon steel by an epoxy resin containing organically modified clay, *Surface and Coatings Technology* 201(16-17) 7408–7415(2007).

[29] Yeh J.M., Huang H.Y., Chen C.L., Su W.F., and Yu Y.H., Siloxane-modified epoxy resin-clay nanocomposite coatings with advanced anticorrosive properties prepared by a solution dispersion approach, *Surface and Coatings Technology* 200 2753–2763(2006).

[30] Mandour, H. S., Abdel-Karim, A. M., & Fathi, A. M. Inhibition Efficiency of Copper Corrosion in a Neutral Chloride Solution by Barbituric and Thiobarbituric Acids. *Portugaliae Electrochimica Acta* 39, 85-103 (2021).